

Temperature-dependent magnetoresistance of pure aluminum and dilute Al-Ga and Al-Mg alloys*

M. L. Snodgrass, F. J. Blatt, Jon L. Opsal, and C. K. Chiang[†]

Department of Physics, Michigan State University, East Lansing, Michigan 48824

(Received 18 August 1975)

We have measured the resistance of very pure polycrystalline aluminum wires (resistance ratio ~ 2000) and dilute Al-Ga and Al-Mg alloys in zero field and transverse magnetic fields up to 50 kG for temperatures between 4.2 and 100 K. For all of our samples at low fields, the magnetoresistance, $\Delta\rho/\rho_0$, decreases monotonically with temperature and Kohler's rule is observed. At high fields, however, departures from Kohler's rule are observed. For the pure aluminum samples and with $H > 10$ kG, $\Delta\rho/\rho_0$ first increases with temperature, reaches a maximum at 20–25 K, then decreases monotonically with temperature. The temperature at which the maximum in $\Delta\rho/\rho_0$ occurs increases with increasing field from about 20 K at $H = 10$ kG to about 25 K at $H = 50$ kG. Also, with increasing field the departures from Kohler's rule become more pronounced. Although greatly reduced, similar departures from Kohler's rule are also observed in Al-Ga samples, and to an even lesser extent in Al-Mg samples. We find that our results can be understood in terms of a simple "two-band" model assuming the resistivity of the i th band is of the form $a_i + b_i T^{x_i}$ and the total conductivity is the sum of the conductivities from each band.

I. INTRODUCTION

Kohler's rule^{1,2} states that for a given metal the relative change in resistivity $\Delta\rho/\rho_0$ in a magnetic field H is a universal function of H/ρ_0 , where ρ_0 is the zero-field resistivity at the temperature in question. This result follows from the Boltzmann equation by assuming that the scattering can be characterized by a relaxation time, and it is generally in rough accord with observation. But Kohler's rule cannot claim general validity on either theoretical or experimental grounds, and in fact large deviations from it have been observed in pure aluminum at low temperatures and high magnetic fields.^{3–13}

We have extended these previous observations in order to make a more detailed examination of the deviations from Kohler's rule. In particular we were interested in studying the temperature dependence of $\Delta\rho/\rho_0$, since that is where the deviations are the most striking and yet where there is the least data.

In order to study deviations from Kohler's rule, we have measured the resistance of high-purity polycrystalline aluminum wires in zero-field and in transverse magnetic fields at a number of temperatures from 4.2 to 100 K. The apparatus and experimental technique used in these measurements are described in Sec. II and a summary of the data appears in Sec. III. The results can be understood in terms of a two-band model of conduction, as shown in Sec. IV. Finally, in Sec. V, we summarize our observations and present our conclusions.

II. EXPERIMENTAL TECHNIQUE

A. Apparatus

The cryostat consisted of a vacuum can containing a cylindrical oxygen-free high-conductivity

copper heating block thermally isolated from the liquid-helium bath. The copper heating block was aligned with the bore of a conventional superconducting solenoid. Field homogeneity was 2% over the specimen region for all fields up to the maximum of 50 kG. Specimens were helically wound on the heating block so that the magnetic field would be transverse to the electrical current in the specimens.

With the vacuum can evacuated, the temperature of the heating block and specimen could be raised above the temperature of the liquid-helium bath by applying current to a coil inside the heating block. Temperature measurements were made using a system of Chromel-P vs Au-0.07 at. % Fe thermocouples and the magnetic field effect on the thermocouples are described in an earlier publication.¹⁴ One thermocouple was used to directly measure the temperature of the heating block and specimen. The other thermocouple was incorporated into the feedback loop of the heater's current supply control, so that the thermocouple emf, and thus the temperature, could be brought to any desired value. Once equilibrium was established, this temperature could be maintained within 0.1 K for an arbitrary length of time.

In practice the specimen was initially cooled to 4.2 K by admitting helium exchange gas and allowing the system to equilibrate with the liquid-helium bath. Then the gas was evacuated and measurements were made at successively higher temperatures, up to 100 K.

B. Specimens

Table I gives a summary of several properties of the specimens. All of the samples, except the "zone-refined Al," were made up from the same

TABLE I. Characteristics of the polycrystalline aluminum wires. All specimens except the "zone-refined Al" were made from the same lot of aluminum. Concentrations of the impurities were determined from the masses of aluminum and impurity mixed to form the specimen. Length is the distance between the points where the potential leads were connected. RRR is the residual resistance ratio $R(295\text{ K})/R(4.2\text{ K})$. The zero-field resistivity ρ_0 is determined by calculating A/L from $\rho_0(295\text{ K}) = 2.74\ \mu\Omega\text{ cm}$.

Sample designation	Diameter (mm)	Length (cm)	RRR	$\rho_0(4.2\text{ K})$ ($\eta\Omega\text{ cm}$)
zone-refined Al	0.81	150	1750	1.57
pure Al	1.02	117	1958	1.40
pure Al	2.59	174	1968	1.39
plus 100-ppm Ga	0.51	101	725	3.78
plus 250-ppm Ga	0.51	137	472	5.81
plus 50-ppm Mg	0.51	78	830	3.30
plus 100-ppm Mg	0.51	86	530	5.17
plus 200-ppm Mg	0.51	92	281	9.75
plus 500-ppm Mg	0.51	93	128	21.4

lot of Cominco 99.9999% pure aluminum. The specimens doped with impurities were made by adding either Alcoa 99.9999% pure gallium or Dow triple-sublimed magnesium in an amount sufficient to provide ~ 500 ppm impurity by weight. Less concentrated alloys were prepared by diluting the master alloys with more pure aluminum.

The pure aluminum was etched first with KOH, then with Tucker's etch. The impurities were etched with 10% acetic acid. The metals were melted, mixed, and poured in $\frac{1}{4}$ atm of argon. The slugs were rolled down to wires using tungsten oxide dies for diameters above 0.80 mm, then diamond dies for smaller diameters. For the sake of comparison with aluminum from another source, a length of Gallard-Schlesinger zone-refined aluminum wire, hard-drawn to 0.81 mm, was used as received.

In order to minimize cold working, the samples were wound in a helical configuration on the copper heating block, then removed and cleaned by etching with KOH and washing with water and ethanol. The cleaned specimen was placed on a cylindrical graphite form of the same diameter as the heating block, and annealed for 4 h at 425°C in high vacuum ($<10^{-4}$ Torr), followed by a furnace cool overnight at high vacuum. Finally, the annealed sample was rinsed with ethanol before mounting. The graphite form was cleaned and outgassed at 900°C before each use.

The copper heating block was electrically isolated from the specimen by a layer of cigaret paper and GE 7031 varnish. The specimen was anchored to the heating block by covering it with more varnish. Voltage and current leads were attached to the sample by winding several times and then soldering, using Indalloy No. 3 flux and No. 9

solder. This type of contact proved reliable upon repeated cycling from room temperature to 4.2 K. Since the soldering was performed after the central portion of the sample was anchored with varnish, only the small portions of the specimens near the ends suffered much cold working.

C. Magnetoresistance measurements

The magnetoresistance measurements were made by passing a steady current (typically 100–200 mA) through the specimen and recording the resulting potential drop along the specimen with a digital voltmeter sensitive to 10 nV. To cancel the effects of thermal emfs in the voltage leads, measurements were made with the current flowing in both directions through the sample.

Data representing the temperature and magnetic field dependence of the resistance were taken in the following manner. With the magnetic field fixed, the resistance was measured at a series of temperatures from 4.2 to 100 K. Then the sample was returned to 4.2 K, and the resistance at 4.2 K was checked to ensure no changes due to thermal cycling had occurred. The magnetic field was then fixed at a new value and the process repeated, until data had been collected at 0, 2, 5, 10, 20, 30, 40, and 50 kG.

The measured zero-field resistivity of each specimen was determined by calculating the ratio of cross-sectional area to length (A/L) from the room-temperature resistance using Meaden's¹⁵ value $\rho_0(295\text{ K}) = 2.74\ \mu\Omega\text{ cm}$. This number and the measured resistance at the temperature of interest were then used to compute the resistivity.

Mounting the specimens in a helical configuration introduces $\sim 3^\circ$ of error from proper alignment even when the axis of the heating block is accurately parallel to the field. Since transverse measurements on polycrystalline samples are not so sensitive to misalignment effects, we feel this error does not significantly affect the results.

No corrections were made for size-effects since the parameter of interest $\Delta\rho/\rho_0$ is presumably independent of geometrical considerations if the mean free path of an electron is less than the radius of the wire. This condition was satisfied by all of our specimens. In any event, the corrections for size effects to zero-field resistivity are small for our specimens: if we use Fickett's¹⁰ scheme for corrections to ρ_0 , even at 4.2 K the errors were less than 5% for the pure aluminum.

III. RESULTS

A. Deviations from Kohler's rule

According to Kohler's rule a plot of $\Delta\rho/\rho_0$ vs $H\rho_0(295\text{ K})/\rho_0(T)$ aluminum should result in a universal curve independent of specimen purity. Figure 1 shows a

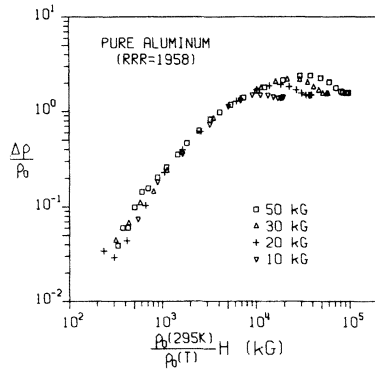


FIG. 1. Kohler plot of data for a single sample of pure aluminum (RRR=1958) at four values of magnetic field. There is considerable deviation from any universal curve in the region of low temperature and high field.

Kohler plot of data taken for a single sample of pure aluminum at four different magnetic fields. Figure 2 shows a Kohler plot of data taken at a fixed field of 50 kG for a series of samples containing small amounts of gallium impurities. As can be seen, Kohler's rule is reasonably valid in the region of high temperature and low field, but it fails in the region of low temperature and high field. The variable H/ρ_0 does not contain all the field and temperature dependence of $\Delta\rho/\rho_0$.

Figure 3 shows a Kohler plot of data taken at a single magnetic field of 50 kG for a series of samples containing small amounts of magnesium impurities. Apparently magnesium impurities tend to reduce the deviations from Kohler's rule in aluminum.

B. Temperature dependence of magnetoresistance

A more interesting way of displaying our results is to plot $\Delta\rho/\rho_0$ as a function of temperature.

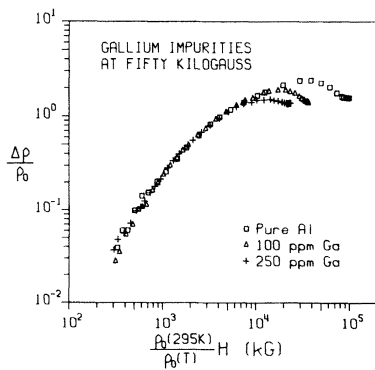


FIG. 2. Kohler plot of data for a series of samples of aluminum with varying concentrations of gallium as an impurity. All of these data were taken at a single magnetic field of 50 kG. As in the previous figure, there is considerable deviation from any universal curve in the region of low temperature and high field.

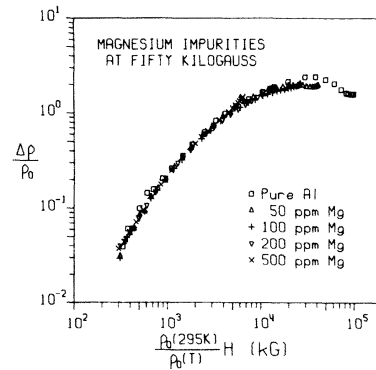


FIG. 3. Kohler plot of data for a series of samples of aluminum with varying concentrations of magnesium as an impurity. All of this data was taken at a single magnetic field of 50 kG. Deviations from a universal curve are less pronounced in this figure than in the previous two.

Figures 4–6 show some of our data plotted in this fashion. The arguments leading to Kohler's rule predict that the magnetoresistance ratio $\Delta\rho/\rho_0$ should exhibit a monotonic decrease with temperature. However, this is not the case with all our data.

Figure 4 displays some of the data for the specimen of pure aluminum with a residual resistance ratio (RRR) of 1958 at several magnetic fields. Similar plots were obtained for other specimens of relatively pure aluminum (i. e., pure Al with an RRR of 1968 and zone-refined Al with an RRR of 1750). As observed by previous investigators,^{3–13} $\Delta\rho/\rho_0$ tends toward saturation with increasing field at low temperatures. However, for higher tempera-

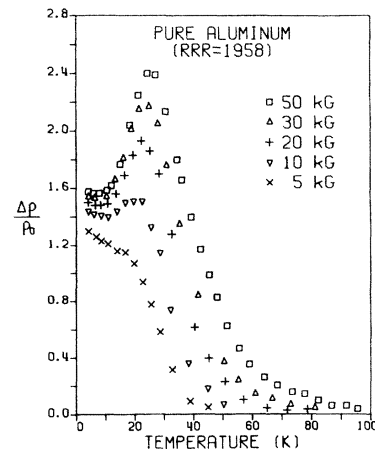


FIG. 4. Magnetoresistance ratio as a function of temperature for a single sample of pure aluminum, at several magnetic fields. For fields of 10 kG or stronger, the magnetoresistance is peaked at a temperature between 20 and 26 K.

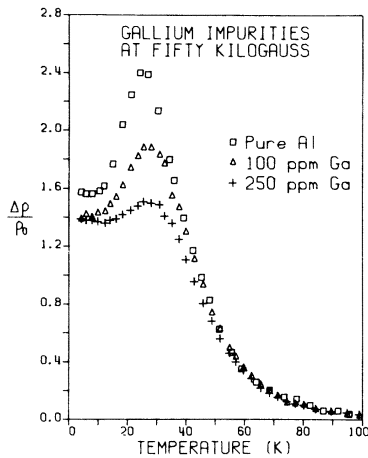


FIG. 5. Magnetoresistance ratio as a function of temperature at a fixed magnetic field (50 kG) for a series of aluminum samples with varying concentrations of gallium impurities. Increasing the concentration of the impurity diminishes the peak in $\Delta\rho/\rho_0$ observed in purer samples.

tures ($T \geq 20$ K) a field as large as 50 kG is no longer sufficient to cause saturation. At low fields $\Delta\rho/\rho_0$ decreases monotonically with increasing temperature, as expected. But for $H \geq 10$ kG, $\Delta\rho/\rho_0$ increases with temperature, reaches a peak near 25 K, then diminishes rapidly with increasing temperature. With increasing magnetic field, the temperature of the maximum in $\Delta\rho/\rho_0$ increases slightly from about 20 K (for $H = 10$ kG) to about 26 K (for $H = 50$ kG). The departures from Kohler's rule are quite pronounced: at 50 kG, $\Delta\rho/\rho_0$ increases from values of 1.6–1.7 at 4.2 K to values of 2.4–2.7 at 26 K (the exact value depending upon which of the three specimens of relatively pure aluminum is in question). Previous investigators have observed even larger deviations in specimens of aluminum with higher RRR, but they had data for only a few temperatures.^{4,7,10}

Although greatly reduced, such deviations from Kohler's rule were also observed in dilute aluminum-gallium alloys. For any single specimen with gallium impurities, plots similar to Fig. 4 result, although the magnitude of $\Delta\rho/\rho_0$ is reduced and there is less tendency towards saturation with H at low temperatures. The data for the gallium alloys are summarized in Fig. 5 which displays $\Delta\rho/\rho_0$ versus temperature for several specimens at a single magnetic field of 50 kG. For a given value of magnetic field, increasing the gallium concentration tended to decrease the magnitude of the peak in $\Delta\rho/\rho_0$ and tended to shift the location of the peak to a slightly higher temperature.

Similar comments apply to specimens of dilute aluminum-magnesium alloys, although the tendency

of magnesium to increase $\Delta\rho/\rho_0$ at low temperatures somewhat masks the peak in $\Delta\rho/\rho_0$ near 25 K. The data for the magnesium alloys are summarized in Fig. 6 which displays $\Delta\rho/\rho_0$ versus temperature for several specimens at a single magnetic field of 50 kG.

IV. DISCUSSION

A. Two-band model of aluminum

According to recent models,¹⁶ the three valence electrons of crystalline aluminum are distributed as follows: two of the electrons occupy the first zone and the remaining electron is divided between the second and third zones. The first zone is completely full and contains none of the Fermi surface. The second zone appears as a pocket of holes and contains most of the remaining electron density. The third zone is a complicated "monster" of electrons and has a relatively small electron density.

The Fermi surface is divided between the second and third zones. Since at the temperatures of interest essentially all of the conduction is due to charge carriers near the Fermi surface, we can ignore the first zone in aluminum and treat conduction as a two-band problem. A first approximation (which we use here) is to consider these as independent isotropic bands.

B. Magnetoresistance in two-band model

Expressions for magnetoresistance based on the two-band model have been developed for some time.^{2,17,18} We assume that the total zero-field conductivity σ_0 is just the algebraic sum of the zero-field conductivities in the hole band and in

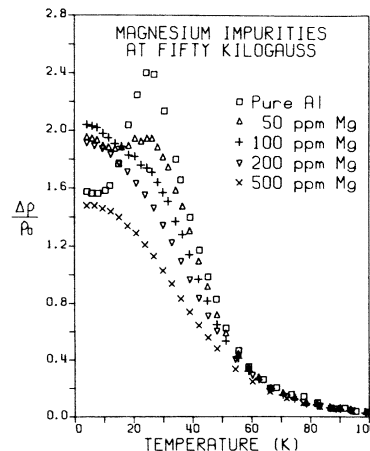


FIG. 6. Magnetoresistance ratio as a function of temperature at a fixed magnetic field (50 kG) for a series of aluminum samples with varying concentrations of magnesium impurities. Increasing the concentration of the impurity tends to obscure the peak in $\Delta\rho/\rho_0$ observed in purer samples.

the electron band:

$$\sigma_0 = \sigma_h + \sigma_e . \quad (1)$$

We then ask how the current in each band is deflected by the application of a magnetic field transverse to the total current. The resulting field-dependent resistivity ρ_H is expressed in terms of the vector sum of the currents and the applied fields. When compared to the zero-field resistivity ρ_0 , we find

$$\frac{\Delta\rho}{\rho_0} = \frac{\rho_H - \rho_0}{\rho_0} = \frac{A}{1 + B[(\rho_0/H)Nec]^2} , \quad (2)$$

where

$$A = \frac{(n_e/n_h + \rho_h/\rho_e)^2}{(\rho_h/\rho_e)(1 - n_e/n_h)^2} \quad (3)$$

and

$$B = \frac{(n_e/N)^2}{(1 - n_e/n_h)^2} \left(\frac{\rho_e + \rho_h}{\rho_0} \right)^2 . \quad (4)$$

We have assumed that in each band the zero-field resistivity is given by

$$1/\rho_i = \sigma_i = n_i e^2 \tau_i / m_i \quad (5)$$

(for $i = e, h$) where, for the i th band, n_i is the carrier density, τ_i is an isotropic relaxation time, and m_i is the effective mass of the charge carrier. Since the total electron density of the two bands corresponds to one electron per atom, we expect $n_h - n_e = N$, where N is the atomic density of crystalline aluminum.

C. Kohler's rule in two-band model

If the relaxation times in the two bands always have the same ratio, then ρ_h/ρ_e is a constant independent of temperature. This implies that the expressions for A and B used in Eq. (2) are also constants. Thus the magnetoresistance is a universal function of H/ρ_0 , which is just Kohler's rule. Furthermore, we expect a monotonic decrease in $\Delta\rho/\rho_0$ as temperature (and ρ_0) increases.

What happens if we no longer assume that ρ_h/ρ_e is constant? Suppose that the resistivity in each band obeys a simplified Matthiessen's rule,

$$\rho_i = a_i + b_i T^{x_i} \quad (6)$$

(for $i = e, h$), where a_i , b_i , and x_i are constants. Then if $a_h/a_e \neq b_h T^{x_h}/b_e T^{x_e}$, we see that ρ_h/ρ_e is not constant and that A and B in Eq. (2) are functions of temperature. By proper adjustment of the parameters a_i , b_i , x_i , and n_i we can get $\Delta\rho/\rho_0$ to display a maximum at a temperature near 25 K.

D. Two-band model fit to experimental data

In our specimens of pure aluminum, for temperatures up to 100 K, the zero-field resistivity roughly obeys the following form:

$$\rho_0 \approx a + bT^x . \quad (7)$$

Since $x = 3.95$ for the pure aluminum with an RRR of 1958, we assumed $x_e = x_h = 3.95$ for all our specimens in order to simplify the data-fitting process. We also applied the constraints that

$$1/a_e + 1/a_h = 1/a \quad (8)$$

and

$$1/b_e + 1/b_h = 1/b . \quad (9)$$

The values of a_h/a_e , b_h/b_e , and n_e/n_h were determined from the expression for A in Eq. (3) by fitting to values of $\Delta\rho/\rho_0$ at the saturated high-field limit. Then the magnitudes of a_e , a_h , b_e , and b_h were fixed by applying Eqs. (8) and (9). Finally the magnitudes of n_e and n_h were determined from the expression for B in Eq. (4) by requiring Eq. (2) to exhibit the proper field dependence.

E. Pure aluminum

Figure 7 shows the theoretical curves for $\Delta\rho/\rho_0$ versus temperature fitted to the specimen of pure aluminum with an RRR of 1958. Figure 8 shows the corresponding theoretical curve for ρ_0 versus temperature. Table II gives the parameters used in Eqs. (2) and (6) in order to generate the curves. These parameters were adjusted until reasonably good fits to both ρ_0 and $\Delta\rho/\rho_0$ were obtained for temperatures between 4 and 60 K. As can be seen in the figures, the theoretical curves have the correct qualitative behavior, but agreement with experiment is only semiquantitative. It was not

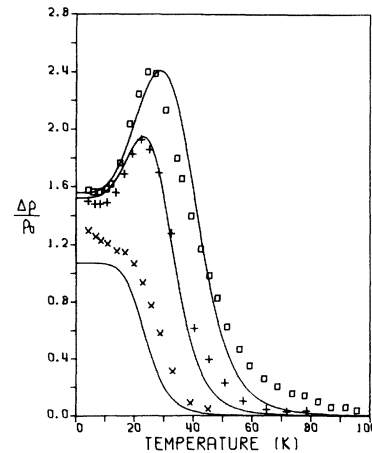


FIG. 7. Theoretical plot of magnetoresistance ratio vs temperature for pure aluminum (RRR=1958) using the two-band model. Curves are shown for three values of magnetic field: 5, 20, 50 kG. The corresponding data points from Fig. 4 are also shown. The parameters used in Eqs. (2) and (6) in order to generate the curves are listed in Table II. The parameters were adjusted until reasonably good fits to data for both ρ_0 and $\Delta\rho/\rho_0$ were obtained for temperatures between 4 and 60 K.

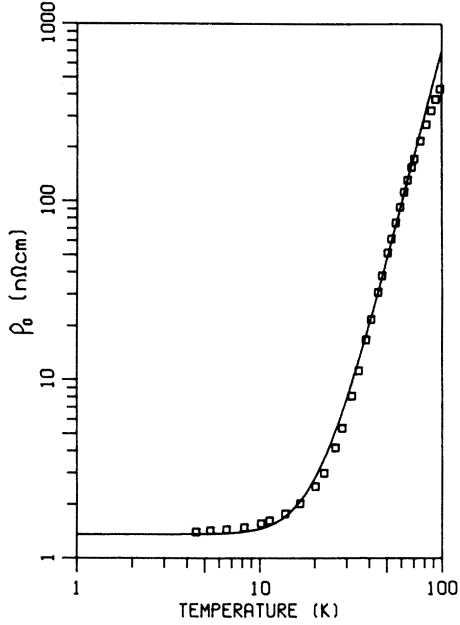


FIG. 8. Zero-field resistivity vs temperature for pure aluminum (RRR=1958). The solid line represents the theoretical curve given by the two-band model, using the parameters of Table II in Eqs. (1) and (6). The data points for the resistivity ρ_0 were obtained from the actual resistance by calculating A/L from the value $\rho_0(295 \text{ K}) = 2.74 \mu\Omega \text{ cm}$.

possible to obtain better agreement between the theoretical curves and experiment, at least not while using the simplified expressions for ρ_i given in Eq. (6) with $x_e = x_h \approx 4$.

The atomic density of aluminum is $N = 6.02 \times 10^{22} \text{ cm}^{-3}$. Using the parameters in Table II, we see that in our model $n_e = 0.47N$ and $n_h = 2.34N$, and therefore $n_h - n_e = 1.87N$. But from models of the Fermi surface and from high-field Hall-effect data,^{19,20} we would expect to have $n_h - n_e = N$. It appears that n_e and n_h are somewhat larger than we would like. This is due to the need to get the proper saturation behavior in the expression for B ; the only other alternative in this model would be to let $n_e = 0.25N$, $n_h = 1.25N$, and require $(\rho_e + \rho_h)$ to be 1.87 times larger than the value needed to fit the zero-field resistivity.

Also the value of n_e/n_h is somewhat larger than most models of the Fermi surface would predict. It is interesting to note that Druyvesteyn²¹ found that he needed a comparable value, $n_e/n_h = 0.167$, when using the two-band model to explain size effects in the magnetoresistance of aluminum.

According to Eq. (5), we expect that the ratio of zero-field resistivities in the two bands will be given by

$$\rho_h/\rho_e = n_e \tau_e m_h / n_h \tau_h m_e. \quad (10)$$

If we take recent data^{22,23} for the cyclotron masses of the electrons and holes we find $m_h/m_e \approx 10$. Using this, along with our value of $n_e/n_h = 0.2$, we see that

$$\rho_h/\rho_e \approx 2\tau_e/\tau_h. \quad (11)$$

At the lowest temperatures our model has $\rho_h/\rho_e \approx 0.526$ so that $\tau_e/\tau_h \approx 0.26$. At temperatures near the peak in $\Delta\rho/\rho_0$ we have $\rho_h/\rho_e \approx 1.26$ so that $\tau_e/\tau_h \approx 0.61$. Even at high temperatures, we have $\rho_h/\rho_e \approx 1.62$ so that $\tau_e/\tau_h \approx 0.81$. Thus over the entire temperature range of interest to us, we have $\tau_e/\tau_h < 1$.

For comparison, at liquid-helium temperatures: from magnetoresistance size-effect data Druyvesteyn²¹ concluded $\rho_h/\rho_e = 0.045$ and $n_e/n_h = 0.167$ so that $\tau_e/\tau_h \approx 0.027$; from Hall-effect data Ashcroft²⁰ concluded that $\tau_e/\tau_h \approx 0.6$; and from thermopower measurements Huebener²⁴ concluded $\tau_e/\tau_h < 1$. Druyvesteyn's value seems a bit extreme, but then he started with the assumption that there was sufficient difference between the relaxation times so that all of the size effects were due to the hole band only. It seems likely that $\tau_e/\tau_h \lesssim 1$ in reasonably pure aluminum at low temperatures.

Although our model qualitatively reproduces most of the characteristics of the experimental curves, it does have at least one shortcoming at low temperatures: the small dip in $\Delta\rho/\rho_0$ between 4 and 15 K at high fields is missing. We found that it was possible to produce such a dip with our model if we no longer assume that $x_e = x_h$. If we assumed $x_h > x_e$ (and correspondingly adjusted the other parameters) we could get something resembling the desired behavior in $\Delta\rho/\rho_0$. However, we did not pursue this scheme of different temperature dependences very far, since it was much more difficult to adjust the other parameters in order to obtain a good fit.

In any case our model assumed a temperature dependence which was probably much too simple. This is apparent in Fig. 7 where $\Delta\rho/\rho_0$ decreases

TABLE II. Parameters used in Eqs. (2) and (6) to generate the theoretical curves shown in Figs. 7 and 8.

a_e	3.93 nΩ cm
a_h	2.07 nΩ cm
b_e	$1.44 \times 10^{-5} \text{ n}\Omega \text{ cm}/\text{K}^{3.95}$
b_h	$2.33 \times 10^{-5} \text{ n}\Omega \text{ cm}/\text{K}^{3.95}$
x_e	3.95
x_h	3.95
n_e	$2.82 \times 10^{22} \text{ cm}^{-3}$
n_h	$14.1 \times 10^{22} \text{ cm}^{-3}$

too rapidly at high temperature. Neither our data, nor that of others,^{25,26} has ρ_0 depending upon T exactly as $a + bT^x$ with $x \approx 4$. For instance, Garland and Bowers²⁷ have reported that the total zero-field resistivity at low temperatures goes as $\rho_0 = \alpha + \beta T^2 + \gamma T^5$. At higher temperatures (but still less than 100 K) the largest exponent of T is considerably less than 5. If we were to assume some more complex scheme for ρ_0 in order to take all these temperature dependences into account, perhaps we would get better results with our model. However, it would be much more difficult to fit the parameters to the data, and it is questionable whether such an attempt would be worthwhile, given the inherent deficiencies of our simple two-band model.

F. Inherent deficiencies of model

Obvious shortcomings of the two-band model as we have applied it are that it ignores the possibility of interband transitions, anisotropic bands, or magnetic breakdown. For example, Kagan and Flerov²⁸ have shown that if there is a temperature-dependent anisotropy in each band, then the actual magnetoresistance will be larger than that predicted by a simple isotropic two-band model. It can be deduced that this will help alleviate the problem of the large values for the densities n_e and n_h , mentioned earlier in this

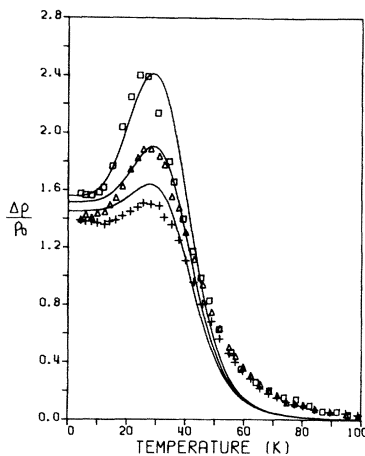


FIG. 9. Theoretical plot of magnetoresistance ratio vs temperature at a constant magnetic field of 50 kG for three specimens of aluminum with varying amounts of gallium impurities (pure Al, 100-ppm Ga, 250-ppm Ga). Corresponding data points from Fig. 5 are also shown. The parameters used in Eqs. (2) and (6) to generate the curve for pure aluminum are the same as in Table II and Figs. 7 and 8. All of the parameters except a_e and a_h are also the same for the curves with impurities. The values of a_e and a_h were adjusted according to the scheme in Eq. (12) and the changes are listed in Table III.

discussion. Unfortunately, there are as yet no detailed models of the temperature-dependent anisotropies in the two bands of aluminum, so we cannot make any reliable attempt at fitting such a model to our data. We might mention, however, that if the anisotropy could change the apparent isotropic resistivities by a factor of order unity (as obtained by Kagan and Flerov), then the density parameters, n_e and n_h , required to fit our data would more nearly correspond to accepted values.

The fact that $\Delta\rho/\rho_0$ never really saturates at high fields, but instead has a small component linear in H (which we have observed), has led many investigators^{3,5,7,8,11,12} to postulate magnetic breakdown at high fields. Our model makes no allowance for such an occurrence. However, the effect is small enough, at least in polycrystalline specimens, that it should not have too much effect on our results.

It is not immediately evident what effect interband transitions would have on the magnetoresistance. However, Ashcroft²⁰ has estimated that interactions between the bands is much less important than scattering completely within each band.

G. Gallium impurities

Figure 9 shows the theoretical curves of $\Delta\rho/\rho_0$ versus temperature for the specimens with gallium impurities. Since gallium is quite similar to aluminum, it seems reasonable, at least at low concentrations, to assume the gallium will not affect the temperature-dependent resistivity in either band and it will not change the ratio of the two temperature-independent resistivities a_e and a_h . Thus, in generating the theoretical curves, the only changes from the parameters in Table II were in a_e and a_h , which we modified according to the scheme

$$a_i(\text{specimen}) = a_i(\text{pure Al}) \times \rho_0(\text{specimen at 4.2 K}) / \rho_0(\text{pure Al at 4.2 K}) \quad (12)$$

for $i = e, h$. Obviously, this scheme just compensates for the change in residual resistance due to the presence of the impurity. These changes are listed in Table III. As can be seen in Fig. 9, this scheme is moderately successful. A slightly better fit can be obtained if a small reduction is made in the ratio a_h/a_e by increasing a_e more than a_h . Apparently gallium in small concentrations affects conduction in aluminum simply by temperature-independent scattering operating nearly equally in each band.

H. Magnesium impurities

The magnetoresistance results for dilute aluminum-magnesium alloys are in some sense anomalous: the addition of magnesium is small concen-

TABLE III. Parameters associated with the theoretical curves shown in Fig. 9. All parameters from Table II are unchanged except a_e and a_h , which were modified according to Eq. (12). Values for a_e and a_h are in units of $n\Omega \text{ cm}$.

Specimen	a_e	a_h	$\frac{\rho_0(\text{specimen at 4.2 K})}{\rho_0(\text{pure Al at 4.2 K})}$
pure Al	3.93	2.07	1.00
plus 100-ppm Ga	10.6	5.59	2.70
plus 250-ppm Ga	16.3	8.58	4.15

trations results in an *increase* in the magnetoresistance at low temperatures.

Such "anomalous" behavior can be understood within the framework of the two-band model as we have employed it here. Whereas the effect of gallium impurities appears to be an increase in the temperature-independent relaxation rates of both bands in proportion to the relaxation rates in nominally pure aluminum, for magnesium impurities it was necessary to modify both the temperature-independent (a_e and a_h) and the temperature-dependent (b_e and b_h) parameters for resistivity in each band. We still assumed that the exponents of T in Eq. (6) and the densities of carriers were unchanged, but we allowed a_e , a_h , b_e , and b_h to change freely until both ρ_0 and $\Delta\rho/\rho_0$ exhibited something near the proper behavior with temperature. Apparently as the concentration of magnesium increases, the ratio a_h/a_e increases and the ratio b_h/b_e decreases. Adjustments to these parameters are listed in Table IV and the resulting theoretical curves are displayed in Fig. 10. (For the sake of clarity, the curves for the specimens with 100 and 200 ppm of Mg are not displayed; they convey little more information than those shown.)

Since magnesium has a different valence than that of aluminum and gallium, it is not too surprising that the simple scheme for adjusting theoretical parameters which worked for gallium im-

TABLE IV. Parameters associated with the theoretical curves shown in Fig. 10. All parameters are unchanged from Table II except a_e , a_h , b_e , and b_h , which were freely adjusted to give a better fit to the data for ρ_0 and $\Delta\rho/\rho_0$. Values for a_e and a_h are in units of $n\Omega \text{ cm}$; values for b_e and b_h are in units of $n\Omega \text{ cm}/\text{K}^{3.95}$.

Specimen	a_e	a_h	b_e	b_h
pure Al	3.93	2.07	1.44×10^{-5}	2.33×10^{-5}
plus 50-ppm Mg	7.28	6.05	1.88×10^{-5}	1.88×10^{-5}
plus 100-ppm Mg	10.7	10.0	2.28×10^{-5}	1.76×10^{-5}
plus 200-ppm Mg	18.9	20.1	2.60×10^{-5}	1.70×10^{-5}
plus 500-ppm Mg	34.9	55.5	2.70×10^{-5}	1.70×10^{-5}

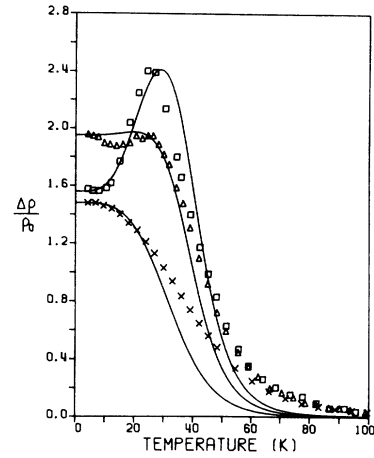


FIG. 10. Theoretical plot of magnetoresistance ratio vs temperature at a constant magnetic field of 50 kG for three specimens of aluminum with varying amounts of magnesium impurities (pure Al, 50-ppm Mg, and 500-ppm Mg). Corresponding data points from Fig. 6 are also shown. The parameters used in Eqs. (2) and (6) to generate the curve for pure aluminum are the same as in Table II and Figs. 7 and 8. However, for the specimens containing the impurities the parameters a_e , a_h , b_e , and b_h were freely adjusted in order to give a better fit to the data for ρ_0 and $\Delta\rho/\rho_0$. Table IV lists the adjustments in these parameters.

purities, fails for magnesium impurities. It would appear that magnesium has quite distinct effects on each of the two conduction bands in this model of aluminum. Increasing the concentration of magnesium apparently increases the temperature-independent impurity scattering much more for the second-zone holes than for the third-zone electrons. At the same time the addition of magnesium also significantly influences the temperature-dependent scattering rates in the two bands: in pure aluminum the phonon-hole relaxation rate is nearly as great as the phonon-electron relaxation rate, but as magnesium is added the phonon-hole scattering rate becomes considerably less than the phonon-electron scattering rate. Although the ratio of scattering times τ_e/τ_h increases at low temperature and decreases at high temperature with increasing concentration of magnesium, upon applying Eq. (11) we note that we still have $\tau_e/\tau_h < 1$ in all of our specimens.

The small dip in $\Delta\rho/\rho_0$ between 4 and 15 K observed experimentally in the specimens of pure aluminum is much more pronounced in the specimen with 50 ppm of magnesium. The failure of our model to produce this dip is once again probably due to the assumption that $x_e = x_h \approx 4$. Since we found it necessary to adjust b_e and b_h in order to get a marginally good fit to the observed data, it seems likely that adjustments in the exponents

of the temperature dependence are probably needed for a better fit. However, we have not pursued this very far, for the reasons mentioned earlier.

In a more realistic model, in which scattering anisotropies are properly taken into account, we would expect markedly different anisotropies associated with scattering from magnesium impurities than for gallium impurities or from phonons.

V. SUMMARY AND CONCLUSIONS

Here is a summary of our experimental observations on high-purity polycrystalline aluminum: (a) $\Delta\rho/\rho_0$ tends toward saturation with H at low T ; (b) a peak in $\Delta\rho/\rho_0$ appears at $T \approx 20\text{--}25$ K for $H > 10$ kG; (c) the location of the peak in $\Delta\rho/\rho_0$ shifts to higher T as H increases; (d) for a given H , increasing the impurity concentration tends to decrease the magnitude of the peak in $\Delta\rho/\rho_0$ and shift its location to a higher T ; (e) particularly at the lowest T , the effect of an impurity is de-

pendent upon its identity; and (f) $\Delta\rho/\rho_0$ falls off roughly as T^{-8} at high T (40–60 K) which is consistent with the simple prediction of Kohler's rule since ρ_0 increases roughly as T^4 in this range.

The simplistic two-band model we have used qualitatively reproduces most of these characteristics of $\Delta\rho/\rho_0$. It seems probable that the mechanism leading to this model accounts for most of the observed transverse magnetoresistance in polycrystalline aluminum. The model results in a ratio of relaxation times τ_e/τ_h which is consistent with other experiments. The densities required to fit $\Delta\rho/\rho_0$ to experiment are too large, but it seems likely that this can be dealt with satisfactorily by modifying the model to take into account anisotropies in each band.

ACKNOWLEDGMENTS

The authors wish to thank B. Shumaker for assistance in sample preparation and J. J. Higgins for helpful discussions.

*Work supported in part by NSF Grant No. GH32954X.

†Present address: Physics Dept., University of Pennsylvania, Philadelphia, PA. 19104.

¹M. Kohler, *Ann. Phys. (N.Y.)* **32**, 211 (1938).

²J. M. Ziman, *Electrons and Phonons* (Clarendon, Oxford, 1960).

³R. J. Balcombe, *Proc. R. Soc. Lond. A* **275**, 113 (1963).

⁴E. S. Borovik, V. G. Volotskaya, and N. Ya. Fogel, *Zh. Eksp. Teor. Fiz.* **45**, 46 (1963) [*Sov. Phys.-JETP* **18**, 34 (1964)].

⁵E. S. Borovik and V. G. Volotskaya, *Zh. Eksp. Teor. Fiz.* **48**, 1554 (1965) [*Sov. Phys.-JETP* **21**, 1041 (1965)].

⁶K. Boning, H. J. Fenzl, E. Olympios, J. M. Welter, and H. Wenzl, *Phys. Status Solidi* **34**, 395 (1969).

⁷Yu. N. Chiang, V. V. Eremenko, and O. G. Shevchenko, *Zh. Eksp. Teor. Fiz.* **57**, 1923 (1969) [*Sov. Phys.-JETP* **30**, 1040 (1970)].

⁸R. J. Balcombe and R. A. Parker, *Philos. Mag.* **21**, 533 (1970).

⁹F. R. Fickett, *Appl. Phys. Lett.* **17**, 525 (1970).

¹⁰F. R. Fickett, *Phys. Rev. B* **3**, 1941 (1971).

¹¹Yu. N. Chiang and O. G. Shevchenko, *Phys. Status Solidi B* **62**, K9 (1974).

¹²J. A. Delaney, *J. Phys. F* **4**, 247 (1974).

¹³W. Kesternich, H. Ullmaier, and W. Schilling, *Philos. Mag.* **31**, 471 (1975).

¹⁴C. K. Chiang, *Rev. Sci. Instrum.* **45**, 985 (1974).

¹⁵G. T. Meaden, *Electrical Resistance of Metals* (Plenum, New York, 1965).

¹⁶A. P. Cracknell, *Adv. Phys.* **18**, 681 (1969).

¹⁷H. Jones, *Proc. R. Soc. Lond. A* **155**, 653 (1936).

¹⁸E. H. Sondheimer and A. H. Wilson, *Proc. R. Soc. Lond. A* **190**, 435 (1947).

¹⁹K. Boning, H. J. Fenzl, J. M. Welter, and H. Wenzl, *Phys. Status Solidi* **40**, 609 (1970).

²⁰N. W. Ashcroft, *Phys. Kondens. Mater.* **9**, 45 (1969).

²¹W. F. Druyvesteyn, *Philos. Mag.* **18**, 11 (1968).

²²C. O. Larson and W. L. Gordon, *Phys. Rev.* **156**, 703 (1967).

²³F. W. Spong and A. F. Kip, *Phys. Rev.* **137**, A431 (1965).

²⁴R. P. Huebener, *Phys. Rev.* **171**, 634 (1968).

²⁵L. A. Hall, *Natl. Bur. Stds. Technical Note No. 365* (U. S. GPO, Washington, D. C., 1968).

²⁶F. R. Fickett, *Cryogenics* **11**, 349 (1971).

²⁷J. C. Garland and R. Bowers, *Phys. Kondens. Mater.* **9**, 36 (1969).

²⁸Yu. N. Kagan and V. N. Flerov, *Zh. Eksp. Teor. Fiz.* **66**, 1374 (1974) [*Sov. Phys.-JETP* **39**, 4 (1974)].